A Multiple-Porosity Method for Simulation of Naturally Fractured Petroleum Reservoirs

Yu-Shu Wu, SPE, Lawrence Berkeley Laboratory
Karsten Pruess, SPE, Lawrence Berkeley Laboratory

Summary. This paper describes the application of the method of "Multiple Interacting Continua" (MINC) to the simulation of oil recovery in naturally fractured reservoirs. A generalization of the double-porosity technique, the MINC method permits a fully transient description of interporosity flow by numerical methods. We present examples to demonstrate the utility of the MINC method for modeling oil-recovery mechanisms by water imbibition and field applications for five-spot waterflooding and water coning problems in fractured reservoirs. All results show that the MINC method provides accurate predictions of the behavior of naturally fractured reservoirs, while requiring only a modest increase in computation work compared with the double-porosity method. The double-porosity method may result in large errors for matrix blocks of low permeability or large size.

Introduction

The study of fluid flow in naturally fractured petroleum reservoirs has been a challenging task. Considerable progress has been made since the 1960's because many fractured hydrocarbon reservoirs have been discovered and put into development in the past decades. Most papers treating flow in fractured reservoirs consider that global flow occurs primarily through the high-permeability, low-effective-porosity fracture system surrounding matrix rock blocks. The matrix blocks contain the majority of the reservoir storage volume and act as local source or sink terms to the fracture system. The fractures are interconnected and provide the main fluid flow path to injection and production wells.[1,2]

Because of the complexity of the pore structure of fractured reservoirs, no universal method for the simulation of reservoir behavior exists. Several different double-porosity models (DPM's) have been developed to describe single-phase and multiphase flow in fractured media.[3-11] Usually, analytic approximations are introduced for the coupling between fracture and matrix continua. For example, it is commonly assumed that a quasisteady state exists in the primary-porosity matrix elements at all times.

Very little work has been done so far in studying transient flow in the matrix blocks or between matrix and fracture systems either numerically or experimentally. As a generalization of the double-porosity concept, Pruess and Narasimhan[7] developed the MINC method, which treats the multiphase and multidimensional transient flow in both fractures and matrix blocks by a numerical approach. This method was successfully applied to a number of geothermal reservoir problems.[6,12,13] The MINC method of Pruess and Narasimhan[7] involves discretization of matrix blocks into a sequence of nested volume elements, which are defined on the basis of distance from the block surface (Fig. 1a). In this way, it is possible to resolve in detail the gradients (of pressure, temperature, etc.) that drive interporosity flow. This discretization technique was later adopted by Gilman[11] for flow in fractured hydrocarbon reservoirs and by Neretnieks and Rasmuson[14] for chemical transport in fractured groundwater systems.

In the present paper, we apply the MINC method to study oil-recovery mechanisms in fractured reservoirs and to obtain insight into the behavior of water/oil flow during the imbibition process. Imbibition is regarded as a very important mechanism of oil production in waterflooding or water coning of fractured reservoirs.[15,16] For multiphase flow, pressure, viscous, gravitational, and capillary forces should all be taken into account. To understand the roles played by the three kinds of forces, we have studied the imbibition process with the MINC method, the conventional DPM, and with a detailed explicit discretization of matrix blocks.

The comparison of the results from the three methods shows that the MINC method can give an accuracy of better than 1% at all times, while the DPM approximation with quasisteady interporosity flow can produce large errors, especially for matrix blocks with low permeability or large size.

We also apply the MINC method to match published data of a five-spot waterflood[4,9] and the observed coning behavior of a well with bottomwater drive in a fractured oil reservoir.[17] Satisfactory results have been obtained for the two examples. In both the imbibition study of individual matrix blocks and field-scale applications, the MINC method is found to give more reliable history matching and behavior predictions for the simulation of fractured reservoir than the conventional DPM.

In most previous analytical or numerical studies of multiphase flow in porous media, it has been taken for granted that the matrix system can be treated as a single continuum with (locally) uniform pressure and fluid saturation distributions. To the best of our knowledge, no studies for multiphase flow have been published concerning how much error will be introduced by this treatment and under what conditions the quasisteady approximation for interporosity flow is acceptable for engineering applications. The applicability of the DPM method is discussed by analyzing the results from individual block imbibition studies and field-scale examples with MINC and DPM in this paper. Through the work of this paper, it is found that the DPM method is often unsuitable for the simulation of oil/water imbibition processes in naturally fractured reservoirs. Depending on reservoir fluid and rock properties, DPM may either overestimate or underestimate imbibition oil recovery from matrix blocks, especially for matrix blocks with low permeability and large size or for high oil viscosity. In some special cases, the results from MINC and DPM calculations are very close, either because of similarities in individual block response predicted from either method or because of the compensatory effect of global flow in the fractures on individual block imbibition response in field-scale modeling. In general, it will be difficult to determine the suitability of DPM for a given reservoir problem. It is suggested that individual matrix imbibition studies be carried out with various possible reservoir parameters with DPM approximation as well as explicit discretization before DPM is applied to actual reservoir simulation. Comparison between DPM and EDM results for individual matrix blocks may provide clues for the accuracy to be expected from the DPM approximation in field studies. When changes in water saturation in the fractures are rapid, as may often happen in coning problems or in response to rate changes, it is usually necessary to account for the transient flow inside the matrix blocks and between matrix and fractures.

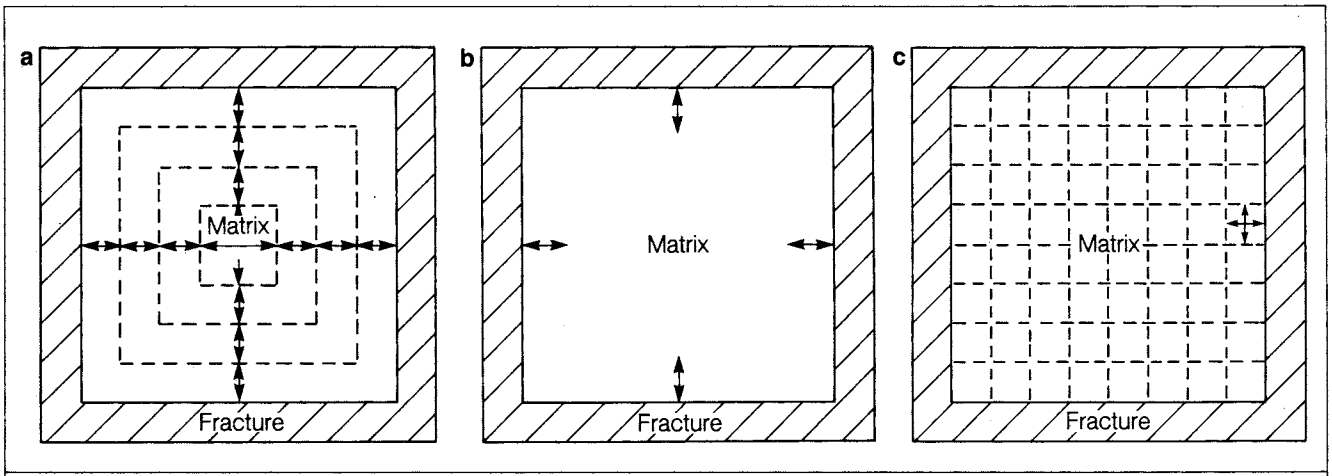

Fig. 1—Discretization of matrix blocks (schematic): (a) MINC, (b) double porosity, (c) explicit discretization.

TABLE 1—RELATIVE PERMEABILITIES AND CAPILLARY PRESSURES FOR DATA SET 1[4]

S_w	k_{rmf}	k_{rof}	P_c (psi)	k_{rwm}	k_{rom}	P_c (psi)
0.000	0.000	1.000	4.000	—	—	—
0.100	0.050	0.770	1.850	—	—	—
0.200	0.110	0.587	0.900	—	—	—
0.250	0.145	0.519	0.725	0.000	0.920	4.000
0.300	0.180	0.450	0.550	0.020	0.705	2.950
0.400	0.260	0.330	0.400	0.055	0.420	1.650
0.500	0.355	0.240	0.290	0.100	0.240	0.850
0.600	0.475	0.173	0.200	0.145	0.110	0.300
0.700	0.585	0.102	0.160	0.200	0.000	0.000
0.800	0.715	0.057	0.110	—	—	—
0.900	0.850	0.021	0.050	—	—	—
1.000	1.000	0.000	0.000	—	—	—

MINC Method

The MINC method, a generalization of the double-porosity technique, is applicable for numerical simulation of heat and multiphase fluid flow in multidimensional fractured porous media. The method permits treatment of multiphase fluids with large and variable compressibility and allows for phase transitions with latent heat effects, as well as for coupling between fluid and heat flow. By dividing the matrix into subdomains, the transient interaction between matrix and fractures is treated in a realistic way. The numerical implementation of the MINC method is accomplished most easily by means of an integral finite-difference formulation.[18]

An important point of the MINC method is the generation of computational grids.[19] A fractured reservoir is at first partitioned into "primary" volume elements (or gridblocks), such as would usually be used for a porous medium. On the basis of the assumption that global flow occurs only through the network of well-connected fractures, the interblock flow connections are then assigned to the fracture continuum. Each primary gridblock is subdivided into a sequence of "secondary" nested volume elements, which are defined on the basis of distance from the matrix block surfaces (Fig.

TABLE 2—PARAMETERS FOR DATA SET 2[9]

S_w	k_{rw}	k_{row}	P_c (psi)
0.200	0.000	1.000	50.00
0.250	0.005	0.860	9.000
0.300	0.010	0.732	2.000
0.350	0.020	0.600	0.500
0.400	0.030	0.492	0.000
0.450	0.045	0.392	− 0.40
0.500	0.060	0.304	− 1.20
0.600	0.110	0.154	− 4.00
0.700	0.185	0.042	− 10.0
0.750	0.230	0.000	− 40.0

Original bubblepoint, psig	5,545
Slope of B_o above p_b, vol/vol-psi	12×10^{-6}
Density of stock-tank oil, lbm/ft^3	51.14
Slope of μ_o above p_b, cp/psi	17.2×10^{-6}
Gas density at standard conditions, lbm/ft^3	0.058
Water FVF, psig	1.07
Water compressibility, vol/vol-psi	3.5×10^{-6}
Water viscosity, cp	0.35
Water density at standard conditions, lbm/ft^3	65
Matrix compressibility, vol/vol-psi	3.5×10^{-6}
Fracture compressibility, vol/vol-psi	3.5×10^{-6}
Matrix permeability, md	1
Matrix porosity, %	30

TABLE 3—PARAMETERS FOR DATA SET 3 (Southern California Oil Field)

S_w	k_{rwm}	k_{rom}	P_c (psi)
0.000	1.000	0.000	356.66
0.037	0.850	0.000	141.69
0.040	0.840	9.42×10^{-11}	124.26
0.049	0.811	2.41×10^{-8}	105.77
0.059	0.779	2.72×10^{-7}	88.27
0.073	0.735	1.95×10^{-6}	70.85
0.095	0.671	1.32×10^{-5}	53.42
0.099	0.659	1.72×10^{-5}	51.77
0.133	0.568	9.85×10^{-5}	35.92
0.201	0.411	8.41×10^{-4}	21.54
0.259	0.303	2.82×10^{-3}	14.38
0.351	0.173	1.13×10^{-2}	7.155
0.380	0.142	1.61×10^{-2}	5.668
0.455	0.0786	3.55×10^{-2}	3.082
0.554	0.0285	8.31×10^{-2}	1.643
0.624	0.0104	0.138	1.232
0.800	0.000	0.405	0.872
0.900	0.000	0.677	0.730
1.000	0.000	1.000	0.206

Matrix porosity, %	20
Matrix permeability, md	1
Fracture permeability, md	10,000
Rock compressibility, vol/vol-psi	3×10^{-5}
Initial oil saturation	0.60
Oil density, lbm/ft^3	60.99
Oil viscosity, cp	90

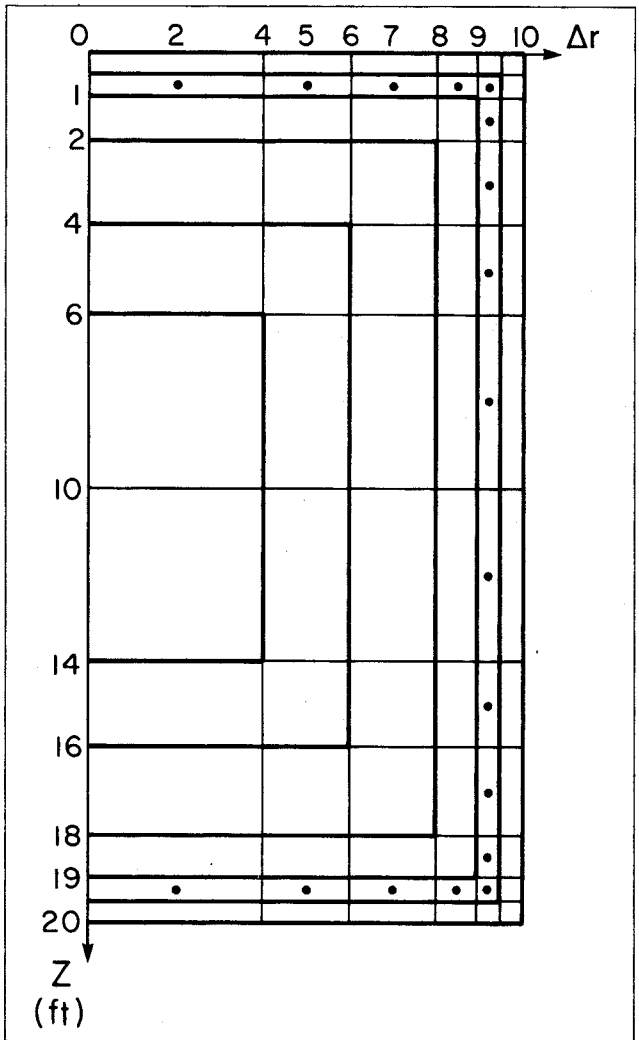

Fig. 2—Discretization of a cylindrical matrix block for MINC and EDM.

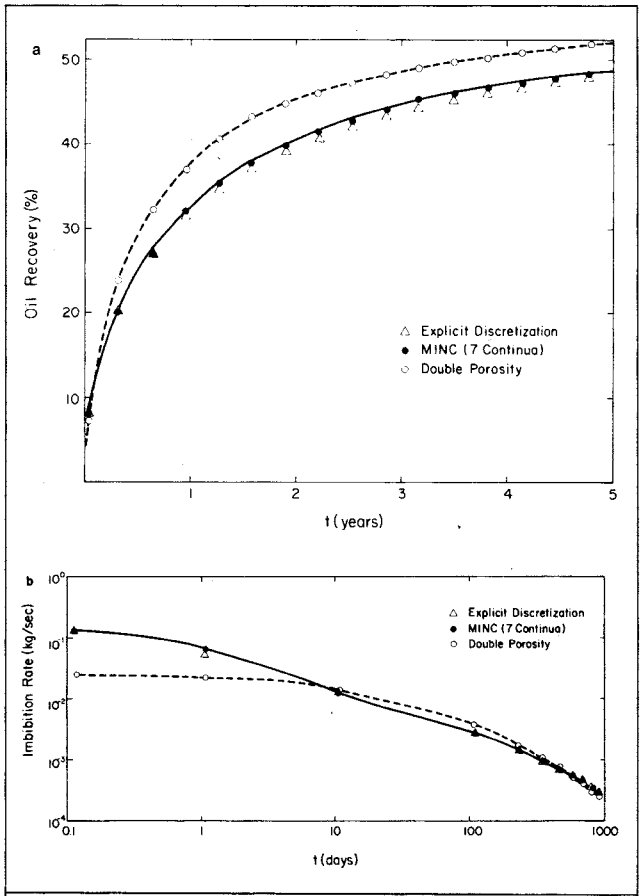

Fig. 3—Imbibition recovery and rate from a cylindrical matrix block—Kazemi *et al.*[4] data): (a) imbibition recovery, (b) imbibition rate.

1a). With these subcontinua, it is possible to represent the transient flow in the matrix blocks and transient interporosity flow between matrix and fractures.

The assumption that global flow occurs only through the fractures breaks down for multiphase systems with strong capillary effects. Depending on overall phase composition, the wetting phase(s) will preferentially occupy the small pores in the rock matrix. while the nonwetting phase(s) will tend to reside in the largest voids, i.e., in the fractures.[20] If the phases tend to be highly segregated between primary and secondary porosity, then global flow of the wetting phase will take place through the primary porosity, crossing fractures at asperity contacts. Furthermore, if there are large density differences between segregated phases, interporosity flow will be subject to strong gravity effects. Such conditions can arise in gas/oil drainage, in water imbibition in large matrix blocks, and in vapor-dominated geothermal reservoirs where the fractures contain only steam while mobile liquid water is present in the matrix blocks.[6] Global matrix/matrix flow and gravity effects in interporosity flow can be described by first discretizing matrix blocks into horizontal layers and then applying nested subregions within each layer.[8]

The MINC method contains the double-porosity approximation as a special case. It can be implemented simply by defining only one matrix continuum and using an appropriate nodal distance for matrix/fracture flow (see Appendix A).

The simulations reported in this paper were carried out with a code STMFLD1,* which solves simultaneous mass-balance equations for two hydrocarbon components and water, as well as a heat balance. STMFLD1 uses an integral finite-difference technique for space discretization and a fully implicit first-order time discretization. The resultant nonlinear algebraic equations are solved by Newton-Raphson iteration that uses a sparse version of LU-decomposition for the set of linear equations arising at each iteration step.[21] STMFLD1 has a capability for simulating thermally enhanced oil recovery in fractured reservoirs, but in the present work was used only for isothermal oil/water two-phase flow.

*Developed by K. Pruess.

Imbibition Oil Recovery

Imbibition displacement of oil by water in relatively tight matrix blocks is a basic oil-recovery mechanism in fractured reservoirs because most of the oil in place is present in the low-permeability matrix system, and flows into the fracture system under viscous, gravity, and capillary forces during oil production. Detailed simulations of individual matrix blocks surrounded by water and oil are presented in this section to study oil-recovery mechanisms and to demonstrate the validity of the MINC method. The MINC results are compared with predictions from DPM and explicit discretization methods (EDM) (see Figs. 1b and 1c). Two kinds of matrix blocks, cubic and cylindrical, are modeled and similar results are obtained. Relative permeability and capillary pressure data and other parameters used are shown in Tables 1 through 3.

Results. EDM is used as a comparison standard for MINC and DPM because EDM can take into account all the mechanisms: viscous, gravity, and capillary effects. Fig. 2 shows a schematic profile of a matrix block of cylindrical shape for MINC and EDM calculations.

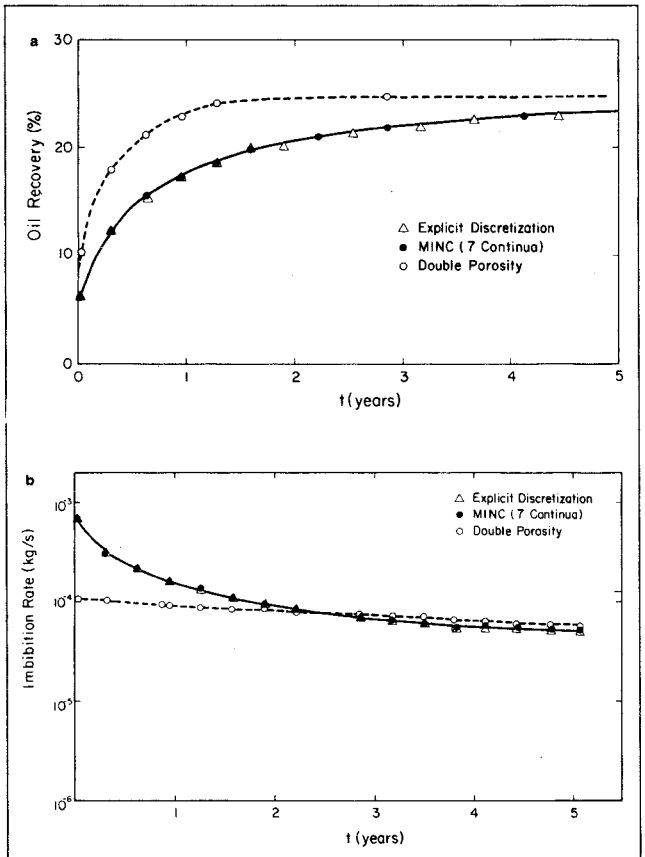

Fig. 4—Imbibition recovery and rate from a cylindrical matrix block—Thomas *et al.*[9] data: (a) imbibition recovery, (b) imbibition rate.

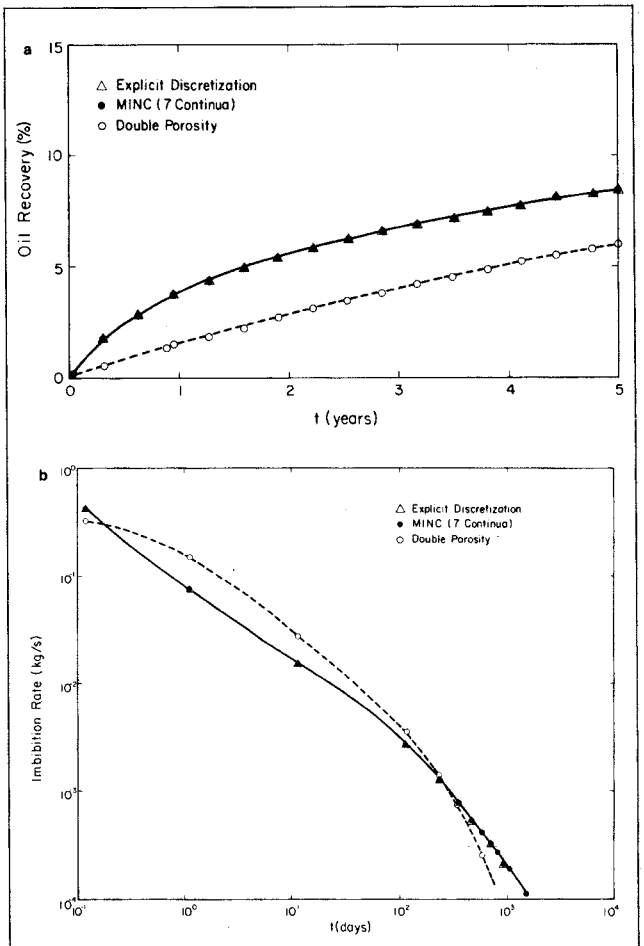

Fig. 5—Imbibition recovery and rate from a cylindrical matrix block—Southern California Field: (a) imbibition recovery, (b) imbibition rate.

Comparisons are shown in Figs. 3 through 5. Oil recovery vs. time is shown in Figs. 3a, 4a, and 5a, calculated from MINC, DPM, and EDM, respectively, for the three data sets given in Tables 1 through 3. In Fig. 6 we present oil-recovery results for a cubic matrix block with the data set of Thomas *et al.*[9] This is virtually identical to the results for a cylindrical block given in Fig. 4a. After many calculations with various matrix sizes and parameters, we have found that there is almost no difference in flow behavior between cubic and cylindrical matrix blocks.

Comparing the oil recovery calculated by the three methods, it can be found that the MINC method is accurate enough to simulate the water/oil imbibition process, while the DPM approach can give very large errors because it neglects transient flow in the matrix. In all cases we have studied, there is excellent agreement between the MINC and EDM results. It is interesting to note that the MINC method requires only a modest increase in computational work compared with DPM because of the one-dimensional treatment of flow in the matrix and saves much more computer time and storage than EDM.

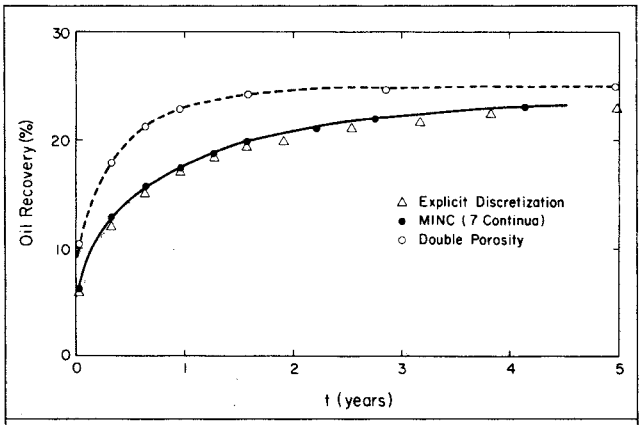

Fig. 6—Imbibition recovery from a cubic matrix block—Thomas *et al.*[9] data.

As shown in Figs. 3 through 6, there is a large difference in oil recovery between the MINC (or EDM) and DPM results. From the curve of imbibition rates (flow rate of oil from matrix into fractures) vs. time in Figs. 3b, 4b, and 5b, the cause of the difference is apparent. The imbibition rates are quite different between the two methods at early time because DPM underestimates the capillary gradient near the matrix block surface. In fact, in DPM the initial differences in capillary pressures between matrix and fractures are assumed to occur over a quasisteady flow distance, d, which is much larger than the nodal distance we use for the first matrix continuum in the MINC method (see Appendix A). Subsequently, the MINC method predicts a buildup of water saturation near the matrix block surface, which diminishes the capillary pressure gradient driving interporosity flow, as well as oil relative permeability. This results in a steeper decline in imbibition rate than that predicted from the DPM approximation, in which all saturation changes are averaged over the entire matrix block. Therefore, at intermediate times, DPM overpredicts imbibition rates. Eventually, for very large times, the DPM imbibition rates decline below the MINC predictions. This occurs simply because for $t \to \infty$, all approximations must converge to the same total oil recovery, corresponding to attainment of capillary equilibrium between matrix and fractures. The relative lengths of the early, intermediate, and late time periods and the magnitude of deviation between MINC and DPM depend on formation parameters, PVT properties, and initial conditions.

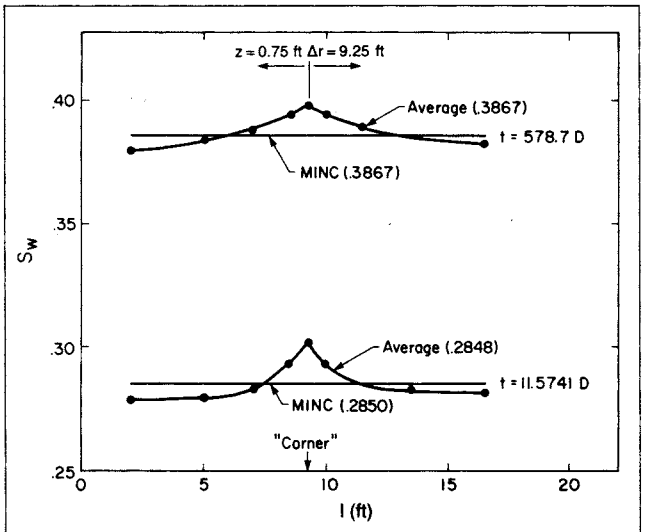

Fig. 7—Saturation distribution in a cylindrical matrix block.

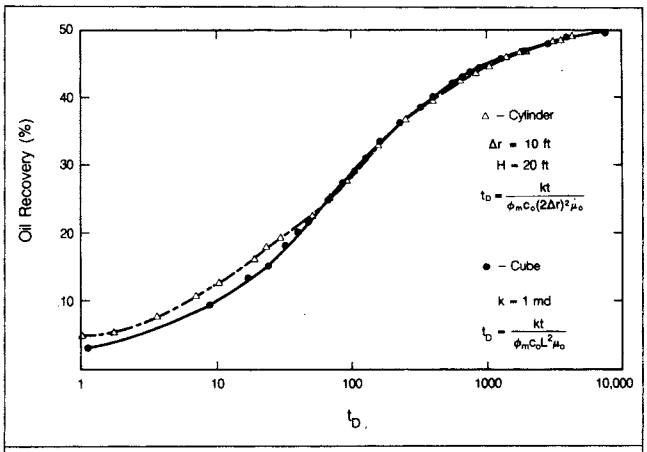

Fig. 8—Effect of matrix block size and rock absolute permeability on imbibition oil recovery vs. dimensionless time.

The agreement between MINC and EDM is excellent throughout. This is further substantiated in Fig. 7, which compares the water saturations calculated in MINC approximation for a certain distance from the surface of a cylindrical block (see Fig. 2) with the detailed predictions of EDM. It is seen that the MINC method underpredicts water saturations near the "corners," where imbibition effects through the cylinder mantle overlap with those through the upper (or lower) cylinder surface. Away from the corners, imbibition effects are slightly overpredicted by the MINC method. The deviations are such that the saturations computed in MINC approximation agree extremely well with the average saturation at a given distance from the block surface obtained in EDM. Fig. 7 shows that this holds true even when gravity effects are included as long as saturations are uniform over the block surface. This result confirms a theoretical prediction by Pruess.[19]

Effects of Matrix Block Size and Permeability. In Appendix B, we show that as far as interporosity flow is concerned, a change in linear matrix block size by a factor α is equivalent to a change in block permeability by a factor $1/\alpha^2$, provided that gravity effects are small compared with capillary effects. We have verified this by comparing calculations for cylindrical and cube-shaped matrix blocks of widely different permeabilities and sizes. This result makes it possible to plot imbibition oil recovery in terms of a dimensionless time, t_D, which is proportional to $(k/L^2)t$ (see Fig. 8).

One of the most difficult problems in history matching and performance prediction of fractured reservoirs is to determine the matrix block size. It cannot be measured directly, so the parameter usually has to be established after tedious history-matching calculations. The equivalence between changes in matrix block size and permeability facilitates practical application of the MINC method to actual reservoir problems and history matching. A computational grid for a MINC model of a flow system needs to be generated only once for a given matrix block shape; changes in matrix block sizes can then be implemented simply by appropriate adjustments in matrix permeability.

The same holds true when considering not just one kind of block shape but a distribution of block shapes and sizes based on some stochastic fracture distribution. As was shown by Pruess and Karasaki,[22] the effective shape of a distribution of block sizes can be conveniently represented by means of a "proximity function" PROX(x), which represents the fraction of matrix material present within a distance x from the fractures. Knowledge of the proximity function is sufficient for defining all geometric parameters of a computational grid in the MINC method. On the basis of the discussion in Appendix B, it is clear that scaling of all matrix block dimensions in any distribution of shapes and sizes by a factor α will be equivalent to a change in matrix block permeability by a factor $1/\alpha^2$ (provided gravity effects in interporosity flow are small).

TABLE 4—DATA FOR FIVE-SPOT PROBLEM OF KAZEMI *et al.*[4]

Initial pressure, psia	3,959.89
Thickness, ft	30
Grid dimensions	8×8
Grid spacing, $\Delta x = \Delta y$, ft	75
Fracture porosity, %	1
Matrix porosity, %	19
Fracture effective permeability, md	500
Matrix permeability, md	1
Matrix shape factor, ft^{-2}	0.08
Water compressibility, vol/vol-psi	3.03×10^{-6}
Bubblepoint pressure, psia	0
Water and oil FVF at bubblepoint, RB/STB	1.0
Slope of B_o above p_b, vol/vol-psi	10.3093×10^{-6}
Fracture compressibility, vol/vol-psi	3×10^{-6}
Water viscosity, cp	0.4444
Water density, psi/ft^3	0.3611
Water injection rate, STB/D	200
Total production rate, STB/D	210

A Five-Spot Example

To demonstrate the application of the MINC method to a field-scale problem, we present a comparison with previous calculations of Kazemi *et al.*[4] and Thomas *et al.*[9] for five-spot waterflood. In this

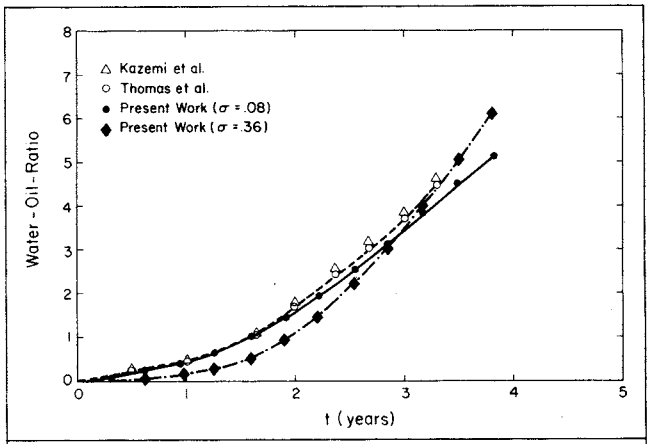

Fig. 9—Kazemi's five-spot problem.

TABLE 5—PARAMETERS FOR THE CONING PROBLEM[16]

Fracture				Matrix			
S_w	k_{rw}	k_{ro}	P_c	S_w	k_{rw}	k_{ro}	P_c
0.0	0.0	1.0	3.869	0.280	0.0	0.940	3.869
0.1	0.052	0.764	1.906	0.324	0.016	0.705	2.773
0.2	0.111	0.592	0.896	0.368	0.034	0.544	2.077
0.3	0.182	0.439	0.540	0.412	0.052	0.431	1.579
0.4	0.271	0.328	0.370	0.456	0.070	0.348	1.195
0.5	0.367	0.239	0.277	0.500	0.092	0.276	0.868
0.6	0.470	0.163	0.205	0.544	0.113	0.207	0.612
0.7	0.586	0.103	0.135	0.588	0.131	0.149	0.384
0.8	0.715	0.057	0.085	0.632	0.154	0.092	0.213
0.9	0.854	0.017	0.043	0.676	0.178	0.034	0.085
1.0	1.0	0.0	0.0	0.720	0.200	0.0	0.0

Perforated thickness, ft	68.2
Thickness of oil zone, ft	369.1
Thickness of water zone, ft	984.2
Well radius, ft	0.328
Well drainage radius, ft	984.2
Radius of the impervious break, ft	439.6

	Fracture	Matrix
Porosity	0.008	0.05
Permeability, md	3,500	5
Compressibility, psi^{-1}	0.0056	0.0
Vertical/horizontal permeability ratio	0.55	
Matrix shape factor, ft^{-2}		0.1068

	Oil	Water
Viscosity, cp	15.8	0.3
Specific gravity	0.8456	1.02
Compressibility, psi^{-1}	4×10^{-6}	0.0
FVF, RB/STB	1.053	1.0

problem, water is injected into one-quarter of a five-spot pattern at a rate of 200 STB/D [31.8 stock-tank m^3/d] and the production rate of total liquid is set at 210 STB/D [33.4 stock-tank m^3/d]. Reservoir dimensions and properties are given in Table 4.

For the treatment of the flow between matrix and fractures, Warren and Root[2] have derived an equation for the shape factor for single-phase flow, σ, based on the quasisteady flow assumption that

$$\sigma=\frac{4N(N+2)}{L^2}, \quad \ldots\ldots\ldots\ldots\ldots\ldots\ldots\ldots\ldots\ldots\ldots\ldots\ldots\ldots (1)$$

where N is number of normal sets of fractures ($N=1$, 2 or 3) and

$$L=\begin{cases} L_x & \text{for } N=1 \\ 2L_xL_y/(L_x+L_y) & \text{for } N=2 \\ 3L_xL_yL_z/(L_xL_y+L_yL_z+L_zL_x) & \text{for } N=3. \end{cases} \quad \ldots\ldots\ldots (2)$$

Kazemi *et al.* and Thomas *et al.* both used the quasisteady approximation, introduced by Warren and Root, and gave different formulas for the matrix shape factor, σ. Kazemi *et al.* proposed

$$\sigma=4\left(\frac{1}{L_x^2}+\frac{1}{L_y^2}+\frac{1}{L_z^2}\right) \quad \ldots\ldots\ldots\ldots\ldots\ldots\ldots\ldots\ldots\ldots\ldots (3)$$

and Thomas *et al.* suggested

$$\sigma=\frac{A}{LV_m}. \quad \ldots\ldots\ldots\ldots\ldots\ldots\ldots\ldots\ldots\ldots\ldots\ldots\ldots\ldots\ldots (4)$$

Note that the shape factors calculated from the above three equations for a cubic matrix block are quite different. As mentioned in the previous sections, the matrix block size makes a difference in flow behavior of imbibition oil displacement and so does the shape factor, because it is related closely to the matrix block size. The simulation results for different σ may lead to remarkable differences in the performance prediction.

In the present five-spot example, Kazemi *et al.* used a value of $\sigma=0.08$[4], which, according to Eq. A-5, corresponds to a nodal distance of $d=5.833$ ft [1.78 m]. A comparison of our simulated WOR's with the results of Kazemi *et al.* and Thomas *et al.*[9] is shown in Fig. 9. For the first 2 years, our calculation using $\sigma=0.08$ is in excellent agreement with the curves of Kazemi *et al.* and Thomas *et al.*, and shows slight deviations at later time. The curve for $\sigma=0.36$ in Fig. 9, based on Warren and Root's shape factor, is lower for the first 3 years and has a more rapid increase during the later production period. We also carried out a MINC calculation for this problem with a discretization of five continua. Surprisingly, the results for produced WOR turned out to be virtually indistinguishable from those obtained in DPM approximation with $\sigma=0.36$, even though the saturation distributions over much of the five-spot pattern are quite different in both cases. How can a transient and a quasisteady approximation for interporosity flow, which give substantially different imbibition response for individual matrix blocks (compare Fig. 3a), end up yielding nearly indistinguishable WOR's in a five-spot flood? The answer is that the aggregate response of many matrix blocks in a flood problem tends to compensate for differences in individual block response. In the present case, the DPM approximation gives more rapid oil recovery from an individual block over virtually the entire period of interest (see Fig. 3a). Therefore, in the DPM calculation, matrix blocks near the injector will take up more water and deliver more oil than predicted from the MINC method, so that blocks farther downstream from the injector will "see" more oil and less water in the fractures. Therefore, those more distant blocks will give smaller imbibition rates. From this consideration, it is clear that there will be a general tendency for aggregate effects of blocks to compensate for differences in individual block response. The fact that this compensation is virtually quantitative in the present case is to be considered fortuitous.

A Coning Problem

In this section, the MINC approximation is used to match the observed coning behavior of a well in the north China oil field. The data have been previously analyzed by Chen,[17] whose basic reservoir model is axially symmetric—the symmetry axis coincides with the well. The upper part of the reservoir is the oil zone, the middle is the transition zone, and the lower part is the water zone. Near the top of the water zone there is a horizontal thin impervious break. The bottomwater is supplied from the lowest surface of the cylinder on which the pressure is maintained at a constant value. The top and the external border of the cylinder are sealed—i.e., there is no flow across the boundaries. The data used are shown in Table 5.

As given in Table 5, Chen used $\sigma=0.1068$, which corresponds to a cubic matrix block with $L=23.7$ ft [7.2 m]. In the history-match simulation, parameters are calibrated from the water-cut data of the first 200 days of production, and the water-cut data after 200 days are used for checking the predicted results.

The results of the history matching and the behavior prediction computed by MINC and DPM from the data of Table 5, respectively, are shown in Fig. 10. Both models give a reasonable match for observed performance; differences between DPM and MINC are small in this case.

On the Validity of DPM

For practical simulation applications it would be preferable to use the simpler DPM approximation whenever possible and to resort to the more complex MINC description only in cases where the accuracy of DPM is poor. In this section, we examine in more detail the conditions for which acceptable accuracy can be attained with the DPM method. The limitations of DPM can be seen best when comparing the temporal evolution of imbibition rates in individual matrix blocks with the more accurate MINC prediction. As was discussed above, one can distinguish three time periods.

Stage 1—An early period in which DPM underpredicts imbibition rate because it underpredicts the capillary gradients at the matrix block surface.

Stage 2—An intermediate period in which DPM overpredicts imbibition rate because it underestimates buildup of water saturation near the matrix block surface.

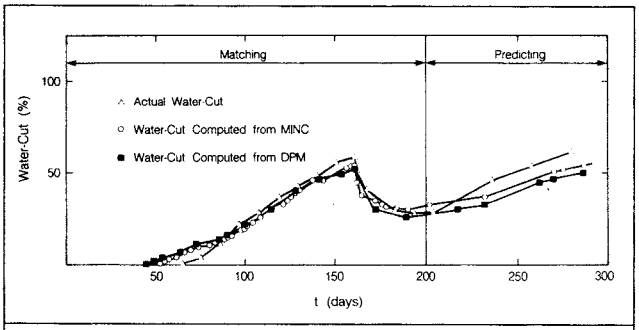

Fig. 10—Chen's coning problem.[17]

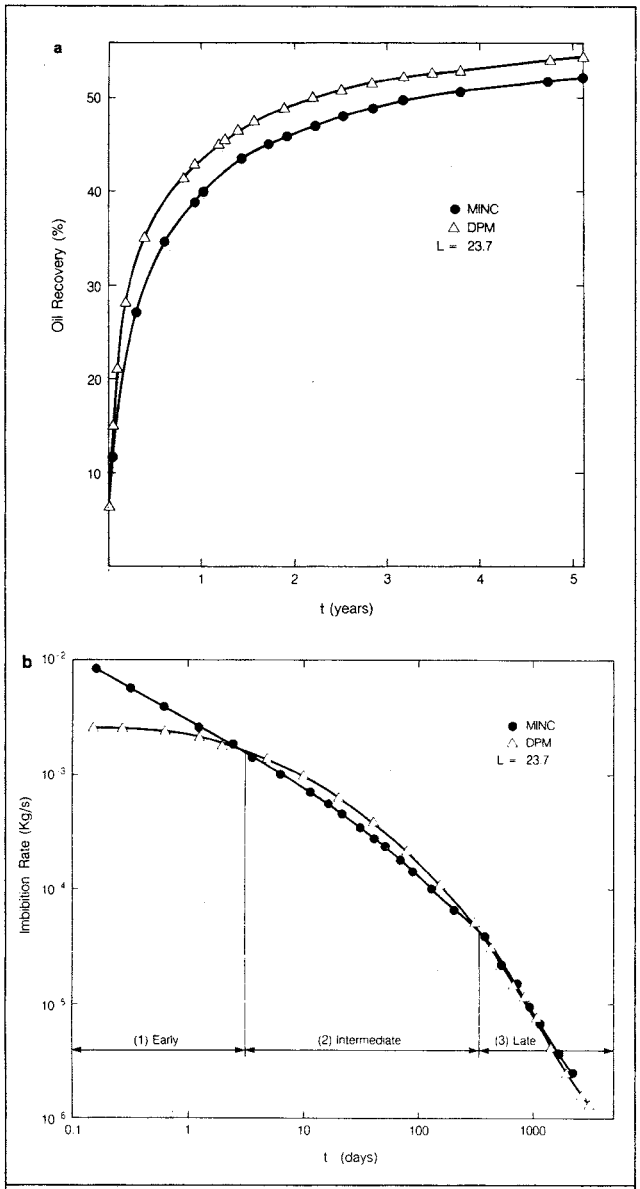

Fig. 11—Imbibition recovery and rate from a cubic matrix block—Chen's data: (a) imbibition recovery, (b) imbibition rate.

Stage 3—A late time period in which DPM again underpredicts imbibition rate because in the intermediate time period (Stage 2) the block has moved closer to eventual capillary equilibrium with the fractures than would be predicted from MINC.

The relative lengths of these time periods and the magnitude of deviation between DPM and MINC in them depend on formation and fluid properties. Generally speaking, differences tend to be larger (DPM less accurate) for small matrix permeability, large matrix block dimensions, large matrix porosity, or large oil viscosity. This can be seen by comparing the imbibition results obtained for Chen's data[17] (Figs. 10 and 11) with those calculated for a modified data set in which matrix permeability was decreased from 5 to 0.1 md and porosity was increased from 5 to 20% (Figs. 12 and 13). For the original data of Chen, most matrix blocks are in the intermediate time period (Stage 2) during the water-coning process, with relatively minor differences between DPM and MINC (see Fig. 11b). For the modified data, most matrix blocks are in Stage 1 (see Fig. 13b), with very large differences between DPM and MINC.

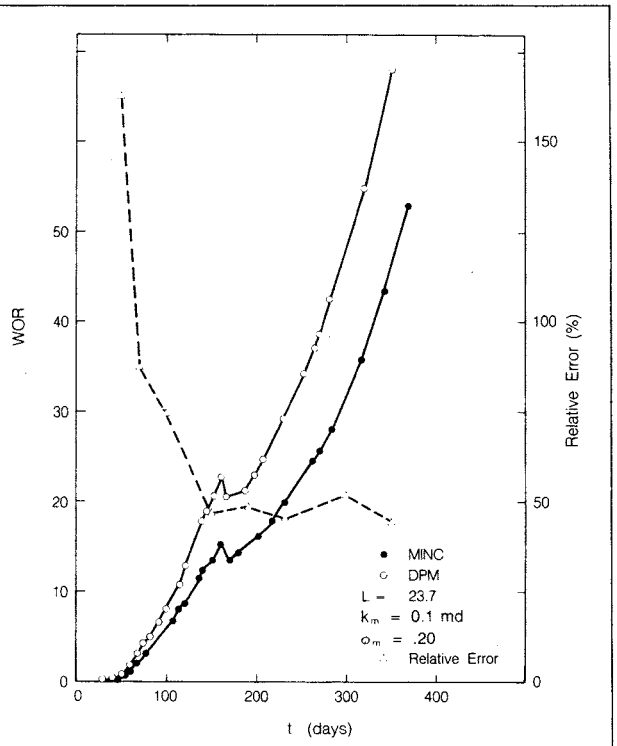

Fig. 12—Comparison of WOR from MINC and DPM—modified Chen's data.

Reservoir response is in general more complicated than individual block response because it involves a superposition of effects from many matrix blocks. Depending on their location in the reservoir relative to the water table and to injection and production wells, different blocks will be at different periods of the imbibition cycle. Aggregate imbibition response of many blocks in a reservoir may be similar in DPM and MINC, even if individual block responses are rather different. This behavior was observed in our simulations of Kazemi's five-spot waterflood example, where DPM and MINC gave virtually indistinguishable results even though individual block response predicted from DPM differs considerably from the MINC results (Figs. 14a and 14b). The explanation is that, with time, the matrix blocks near the injector move into Stage 2 or 3 of the imbibition cycle, while the blocks closer to the production well remain in Stage 1 for a longer time. Overall reservoir response then tends to average out the differences existing in each stage.

For practical reservoir simulation problems, it would be desirable to be able to evaluate the accuracy to be expected from DPM without actually going through a reservoir-wide MINC calculation. It may be possible to accomplish this by plotting individual block imbibition data as shown in Fig. 15. Here we have shown the ratio of recovery predictions from MINC and DPM as a function of total recovery. This presentation of the data removes the somewhat spurious dependence on real (physical) time, instead emphasizing the connection between total recovery and accuracy of DPM. (Note that an explicit discretization calculation for an individual block could be used instead of the MINC calculation with virtually indistinguishable results.) Fig. 15 shows why DPM for the modified

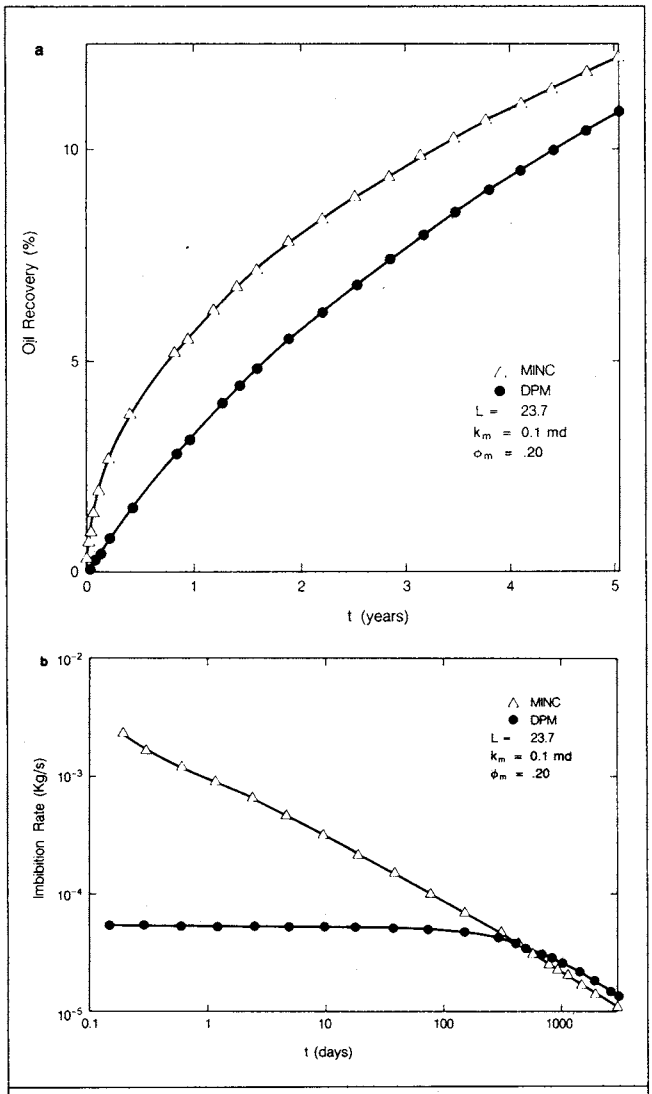

Fig. 13—Imbibition recovery and rate from a cubic matrix block—modified Chen's data: (a) imbibition recovery, (b) imbibition rate.

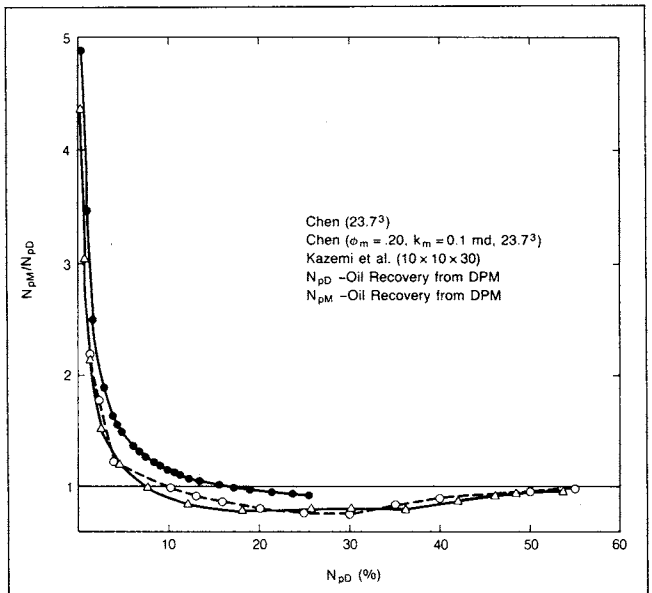

Fig. 15—Comparison of imbibition oil recovery from MINC and DPM.

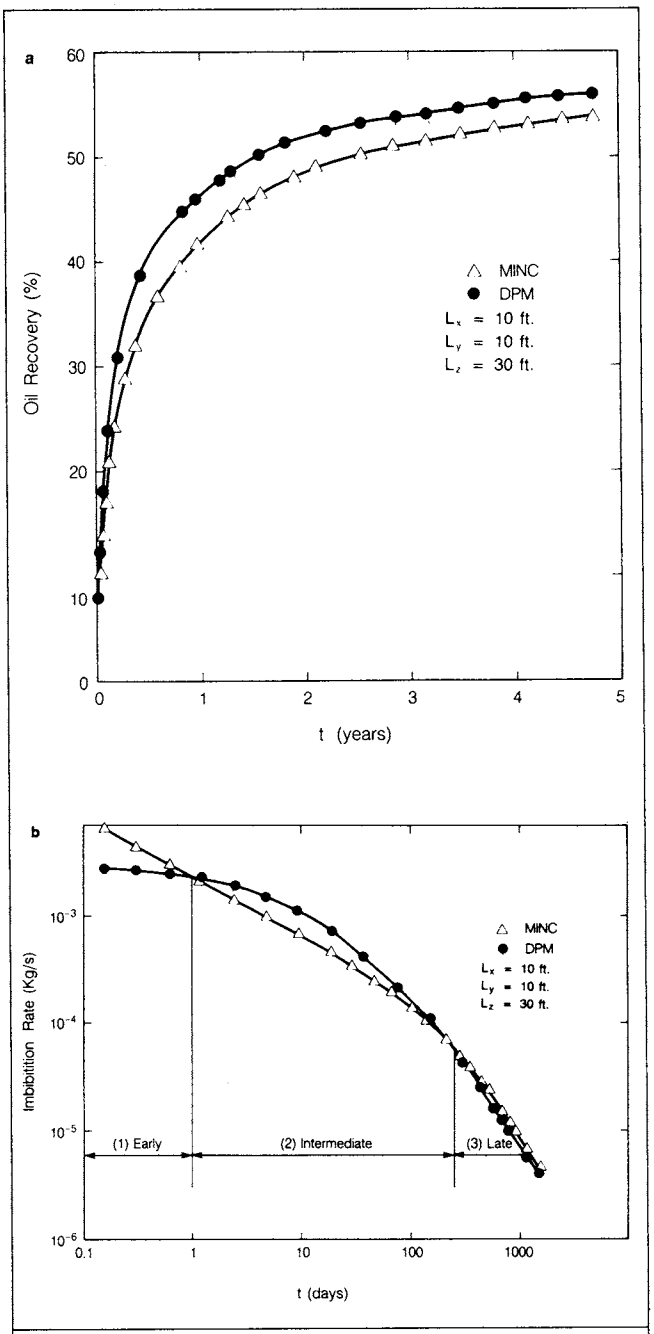

Fig. 14—Imbibition recovery and rate from a rectangular matrix block as used in five-spot example: (a) imbibition recovery, (b) imbibition rate.

data of Chen strongly underestimates oil recovery (overestimates WOR): all matrix blocks are in conditions that plot above $N_{pM}/N_{pD}=1$. For Chen's original data, as well as for Kazemi's data, the N_{pM}/N_{pD} ratio reaches 1 for substantially smaller oil recovery. In these cases, therefore, some matrix blocks will have $N_{pM}/N_{pD}>1$ while others will have $N_{pM}/N_{pD}<1$ after a relatively modest recovery period. In this situation, differences in individual block response will tend to average out, giving a favorable situation for applying DPM.

Conclusions

1. The conventional DPM can give large errors for simulation of oil recovery from individual matrix blocks or from a reservoir by water/oil imbibition mechanisms. The errors increase rapidly with enlargement of matrix blocks or fluid viscosity and with decrease in rock permeability.

2. The MINC method takes into account the transient flow of fluids both in the matrix system and in the fractures. Comparisons

with calculations made with a detailed explicit discretization of matrix blocks have shown that the MINC method gives accurate predictions for water imbibition.

3. Results of five-spot waterflood and coning simulations indicate that the aggregate response of many matrix blocks in a reservoir has a general tendency to compensate for differences in individual block response. This suggests that the DPM with quasisteady approximation for interporosity flow may be applicable even in cases where its basic assumptions are poorly justified.

4. An estimation of the suitability of the DPM approximation for waterflooding and water coning problems can be obtained by comparing quasisteady and transient imbibition predictions for individual matrix blocks.

Nomenclature

A = interface area of matrix block, ft^2 [m^2]
A_{nm} = interface area between Volume Elements n and m, ft^2 [m^2]
B = FVF, bbl/bbl [m^3/m^3]
c = compressibility, psi^{-1} [Pa^{-1}]
d = distance between nodal points, ft [m]
d_J = nodal distance for the innermost matrix node, ft [m]
h = time level index
H = height, ft [m]
i = component index (i=oil, water)
k = absolute matrix permeability, md
k_β = relative permeability to the β phase
l = length coordinate for explicitly discretized matrix block (Fig. 2; $l=\Delta r+Z-0.75$ ft [0.23 m]), ft [m]
L = characteristic dimension of matrix block, ft [m]
L_x = matrix block length, ft [m]
L_y = matrix block width, ft [m]
L_z = matrix block height, ft [m]
M = accumulation term in mass-balance equation, lbm/ft^3 [kg/m^3]
N = number of normal sets of fracture (N=1, 2, or 3)
N_{pD} = oil recovery from DPM, bbl [m^3]
N_{pM} = oil recovery from MINC, bbl [m^3]
p = pressure, psi [Pa]
P_c = capillary pressure, psi [Pa]
Δr = radial distance, ft [m]
S = saturation
t = time, seconds
t_D = dimensionless time
u = mass flux, lbm/ft^2-sec [kg/m$^2\cdot$s]
V_m = matrix-block volume, ft^3 [m^3]
V_n = volume of Gridblock n, ft^3 [m^3]
x = distance between two points in matrix blocks, ft [m]
X = mass fraction
z = vertical distance, ft [m]
α = scale factor (Appendix A)
μ = viscosity, cp [Pa·s]
ρ = mass density of fluid, lbm/ft^3 [kg/m^3]
σ = matrix shape factor, ft^{-2} [m^{-2}]
ϕ = porosity

Subscripts

b = bubblepoint
D = dimensionless
f = fracture
m = matrix
n = index number of volume element
o = oil
r = relative
w = water
β = phase

Acknowledgments

This work was supported, in part, by the Ministry of Education, The People's Republic of China, and the U.S. DOE under Contract No. DE-AC03-76SF00098.

References

1. Barenblatt, G.E., Zheltov, I.P., and Kochina, I.N.: "Basic Concepts in the Theory of Seepage of Homogeneous Liquids in Fissured Rocks," *J. Appl. Math.* (1960) **24,** No. 5, 1286–1303.
2. Warren, J.E. and Root, P.J.: "The Behavior of Naturally Fractured Reservoirs," *SPEJ* (Sept. 1963) 245–55; *Trans.*, AIME, **228.**
3. Kazemi, H.: "Pressure Transient Analysis of Naturally Fractured Reservoirs with Uniform Fracture Distribution," *SPEJ* (Dec. 1969) 451–62; *Trans.*, AIME, **246.**
4. Kazemi, H. *et al.*: "Numerical Simulation of Water-Oil Flow in Naturally Fractured Reservoirs," *SPEJ* (Dec. 1976) 317–26; *Trans.*, AIME, **261.**
5. Duguid, I.O. and Lee, P.C.: "Flow in Fractured Porous Media," *Water Resources Res.* (1977) **13,** No. 3, 558–66.
6. Pruess, K. and Narasimhan, T.N.: "On Fluid Reserves and the Production of Superheated Steam from Fractured, Vapor-Dominated Geothermal Reservoirs," *J. Geophys. Res.* (1982) **87,** No. B11, 9329–39.
7. Pruess, K. and Narasimhan, T.N.: "A Practical Method for Modeling Fluid and Heat Flow in Fractured Porous Media," *SPEJ* (Feb. 1985) 14–26.
8. Pruess, K.: "A Quantitative Model of Vapor-Dominated Geothermal Reservoirs as Heat Pipes in Fractured Porous Rock," *Trans.*, Geothermal Resources Council (1985) **9,** Part II, 353–61.
9. Thomas, L.K., Dixon, T.N., and Pierson, R.G.: "Fractured Reservoir Simulation," *SPEJ* (Feb. 1983) 42–54.
10. Gilman, J.R. and Kazemi, H.: "Improvements in Simulation of Naturally Fractured Reservoir," *SPEJ* (Aug. 1983) 695–707.
11. Gilman, J.R.: "An Efficient Difference Method for Simulating Phase Segregation in the Matrix Blocks in Double-Porosity Reservoirs," *SPERE* (July 1986) 403–13.
12. Pruess, K.: "Heat Transfer in Fractured Geothermal Reservoirs with Boiling," *Water Resources Res.* (Feb. 1983) **19,** No. 1, 201–08.
13. Bodvarsson, G.S., Pruess, K., and O'Sullivan, M.J.: "Injection and Energy Recovery in Fractured Geothermal Reservoirs," *SPEJ* (April 1985) 303–12.
14. Neretnieks, I. and Rasmuson, A.: "An Approach to Modeling Radionuclide Migration in a Medium with Strongly Varying Velocity and Block Sizes Along the Flow Path," *Water Resources Res.* (Dec. 1984) **20,** No. 12, 1823–36.
15. de Swaan, A.: "Theory of Waterflooding in Fractured Reservoirs," *SPEJ* (April 1978) 117–22.
16. Menouar, H. and Knapp, R.M.: "Numerical Simulation of the Imbibition Process in Fractured Reservoirs," paper SPE 9370 presented at the 1980 SPE Annual Technical Conference and Exhibition, Dallas, Sept. 21–24.
17. Chen, H-Z.: "Numerical Simulation of Coning Behavior of a Single Well in a Naturally Fractured Reservoir," *SPEJ* (Dec. 1983) 879–84.
18. Narasimhan, T.N. and Witherspoon, P.A.: "An Integrated Finite Difference Method for Analyzing Fluid Flow in Porous Media," *Water Resources Res.* (1976) **12,** No. 1, 57–64.
19. Pruess, K.: "GMINC—A Mesh Generator for Flow Simulation in Fractured Reservoirs," Report LBL-15227, Lawrence Berkeley Laboratory, Berkeley, CA (March 1983).
20. Wang, J.S.Y. and Narasimhan, T.N.: "Hydrologic Mechanisms Governing Fluid Flow in a Partially Saturated, Fractured, Porous Medium," *Water Resources Res.* (1985) **21,** No. 12, 1861–74.
21. Duff, I.S.: "MA28—A Set of FORTRAN Subroutines for Sparse Unsymmetric Linear Equations," Report R8730, Atomic Energy Research Establishment Harwell, Ditcot, Oxfordshire, England (July 1977).
22. Pruess, K. and Karasaki, K.: "Proximity Functions for Modeling Fluid and Heat Flow in Reservoirs with Stochastic Fracture Distributions," paper presented at the 1982 Stanford U. Workshop on Geothermal Reservoir Engineering, Stanford, Dec. 14–16.

Appendix A—Relationship Between Double-Porosity Matrix Shape Factor and Geometric Parameters of the Integral Finite-Difference Method

Warren and Root[2] wrote a quasisteady approximation for interporosity flow in single-phase conditions as follows:

$$\phi_m c_m \frac{\partial \overline{p_m}}{\partial t} = \sigma \frac{k_m}{\mu} (\overline{p_f} - \overline{p_m}). \quad \text{(A-1)}$$

The overbars indicate averages over matrix and fracture continua, respectively. The parameter σ (Warren and Root used the notation α) is a "matrix shape factor,"[9] which characterizes the matrix block surface area per unit volume.

To obtain the relationship between σ and the geometric parameters used in an integral finite-difference description of interporosity flow, consider the point differential equation for flow in the matrix blocks:

$$\phi_m c_m \frac{\partial p_m}{\partial t} = \nabla \cdot \frac{k_m}{\mu} \nabla p_m. \quad \text{(A-2)}$$

Integrating over one matrix block, we obtain

$$V \phi_m c_m \frac{\partial \overline{p_m}}{\partial t} = A \frac{k_m}{\mu} (\overline{\nabla p_m})_{\text{surface}}. \quad \text{(A-3)}$$

In double-porosity approximation (two continua), the pressure gradient at the block surface is approximated by the following finite-difference expression:

$$(\overline{\nabla p_m})_{\text{surface}} \approx \frac{\overline{p_f} - \overline{p_m}}{d}, \quad \text{(A-4)}$$

with d being the distance of the matrix nodal point from the block surface. Comparing Eqs. A-1, A-3, and A-4, we obtain

$$\sigma = \frac{A}{Vd}. \quad \text{(A-5)}$$

For matrix blocks in the shape of cubes, Warren and Root give $\sigma = 60/L^2$. Noting that $A/V = 6/L$ in this case, we obtain a nodal distance $d = L/10$ for quasisteady flow. Different values of σ proposed for multiphase flow can be accommodated in the integral finite-difference representation by simply calculating the corresponding nodal distance d from Eq. A-5.

Appendix B—Dependence of Interporosity Flow on Matrix Block Size

Let us consider a scale change for the matrix blocks in which all distances between points change by the same common factor,

$$x \rightarrow x' = \alpha x. \quad \text{(B-1)}$$

Such a scale change will not affect the shape of the blocks. To evaluate its effect on interporosity flow, we consider the governing mass-balance equations for matrix/matrix or matrix/fracture flow. Ignoring gravity effects, we have

$$M_n^{ih+1} - M_n^{ih} - \frac{\Delta t}{V_n} \sum_m A_{nm} u_{nm}^i = 0, \quad \text{(B-2)}$$

where

$$u_{nm}^i = -\frac{k}{d_{nm}} \sum_\beta X_\beta^i \frac{k_\beta}{\mu_\beta} \rho_\beta (p_{\beta,m} - p_{\beta,n}). \quad \text{(B-3)}$$

Thus, the permeability and geometry parameters appear in Eq. B-2 in the group,

$$k \frac{A_{nm}}{V_n d_{nm}}. \quad \text{(B-4)}$$

Suppose that the total number of matrix blocks in gridblock V_n is ν. Under the scale change (Eq. B-1) this number will change to $\nu' = \nu/\alpha^3$. The surface area per matrix block will change from A_{nm}/ν to $\alpha^2 A_{nm}/\nu$, so that the total surface area will become

$$A_{nm}' = \nu' \frac{\alpha^2 A_{nm}}{\nu} = \frac{1}{\alpha} A_{nm}. \quad \text{(B-5)}$$

All nodal distances in the matrix will change according to

$$d_{nm}' = \alpha d_{nm}. \quad \text{(B-6)}$$

Note that for a matrix/fracture connection, the same equation holds because the fracture nodal point will be on the block surface, so that the entire group (Eq. B-4) will change as follows:

$$k \frac{A_{nm}'}{V_n d_{nm}'} = \frac{k}{\alpha^2} \frac{A_{nm}}{V_n d_{nm}}. \quad \text{(B-7)}$$

Thus, an increase in linear matrix block size by a factor α is equivalent to a reduction in matrix permeability by a factor α^2. This result holds for arbitrary (fixed) block shapes and, in fact, for arbitrary distributions of block sizes. Nowhere in the above discussion did we need to require matrix block sizes to be identical.

When gravity effects are included, no simple block-size/permeability relationship is possible. For a gravity term in u_{nm}^i, the geometric data would appear in the group

$$k \frac{A_{nm}}{V_n} \rightarrow k \frac{A_{nm}'}{V_n} = \frac{k}{\alpha} \frac{A_{nm}}{V_n}.$$

For gravity contribution to flow, an increase in linear matrix block size by a factor α is equivalent to a decrease in permeability by the same factor. As matrix block sizes increase, therefore, the contribution of pressure forces to flow will diminish more rapidly than the contribution of gravity forces. This indicates that gravity forces may often be unimportant for imbibition in small matrix blocks but may be very important for large matrix blocks.

SI Metric Conversion Factors

bbl	×	1.589 873	E−01	= m^3
cp	×	1.0*	E−03	= Pa·s
ft	×	3.048*	E−01	= m
ft^3	×	2.831 685	E−02	= m^3
lbm/ft^3	×	1.601 846	E+01	= kg/m^3
psi	×	6.894 757	E+00	= kPa
psi^{-1}	×	1.450 377	E−01	= kPa^{-1}

*Conversion factor is exact.

SPERE

Original SPE manuscript received for review April 2, 1986. Paper accepted for publication May 28, 1987. Revised manuscript received July 10, 1987. Paper (SPE 15129) first presented at the 1986 California Regional Meeting held in Oakland, April 2–4.